

Article

The Effects of Asymmetric Diurnal Warming on Vegetation Growth of the Tibetan Plateau over the Past Three Decades

Haoming Xia ¹ , Ainong Li ², Gary Feng ³ , Yang Li ¹ , Yaochen Qin ^{1,*}, Guangbin Lei ² 
and Yaoping Cui ¹ 

¹ College of Environment and Planning, Key Laboratory of Geospatial Technology for Middle and Lower Yellow River Regions, Henan Collaborative Innovation Center of Urban-Rural Coordinated Development, Henan University, Kaifeng 475004, China; xiahm2002@163.com (H.X.); liyanghenu@163.com (L.L.); cuiyp@reis.ac.cn (Y.C.)

² Research Center for Digital Mountain and Remote Sensing Application, Institute of Mountain Hazards and Environment, Chinese Academy of Sciences, Chengdu 610041, China; ainongli@imde.ac.cn (A.L.); leiguangbin@imde.ac.cn (G.L.)

³ United States Department of Agriculture-Agricultural Research Service, Genetics and Sustainable Agriculture Research Unit, Mississippi State, MS 39762, USA, Gary.Feng@ars.usda.gov

* Correspondence: qinyc@henu.edu.cn; Tel.: +86-371-2388-1858

Received: 11 February 2018; Accepted: 5 April 2018; Published: 7 April 2018



Abstract: Temperatures over the past three decades have exhibited an asymmetric warming pattern between night and day throughout the Tibetan Plateau. However, the implications of such diurnally heterogeneous warming on vegetation growth is still poorly understood. In this paper, we evaluate how vegetation growth has responded to daytime and night-time warming at the regional, biome, and pixel scales based on normalized difference vegetation index (NDVI) and meteorological data from 1982 to 2015. We found a persistent increase in the growing seasonal minimum temperature (T_{\min}) and maximum temperature (T_{\max}) over the Tibetan Plateau between 1982–2015, whereas the rate of increase of T_{\min} was 1.7 times that of T_{\max} . After removing the correlations between T_{\min} , precipitation, and solar radiation, we found that the partial correlation between T_{\max} and NDVI was positive in wetter and colder areas and negative in semi-arid and arid regions. In contrast, the partial correlation between T_{\min} and NDVI was positive in high-cold steppe and meadow steppe and negative in montane steppe or wet forest. We also found diverse responses of vegetation type to daytime and night-time warming across the Tibetan Plateau. Our results provide a demonstration for studying regional responses of vegetation to climate extremes under global climate change.

Keywords: climate extremes; global warming; Tibetan Plateau; ecological responses; NDVI3g; partial correlation analysis

1. Introduction

As one of the key environmental factors impacting the spatial and temporal distribution of vegetation ecosystems, temperature changes directly alter the vegetation growth environment. This affects the vegetation growth dynamics and vegetation structure and function [1]. The fifth Assessment Report of the United Nations Intergovernmental Panel on Climate Change (IPCC) noted that the global average temperature is 0.85 °C higher than of 1880. Additionally, the last 30 years may be the warmest 30 years in the northern hemisphere in the past 1400 years [2]. Meanwhile, the rate of global warming is heterogeneous across spatial scales. For example, the rate of warming for coasts, mountains, and high latitudes is relatively high [3]. Global warming also exhibits temporal asymmetry.

For example, the rate of increase of global surface daily minimum temperatures (T_{\min}) is 1.4 times higher than that of the daily maximum temperature (T_{\max}) [3]. This asymmetric day–night warming trend will have a major impact on the carbon uptake and carbon consumption of vegetation globally. The most critical stages of photosynthesis occur primarily during the daytime so the process is more sensitive to changes in T_{\max} . However, respiration can occur day and night so it is sensitive to both T_{\max} and T_{\min} [4]. While increases in T_{\min} enhance both the respiration of vegetation and carbon consumption, increased photosynthesis during the daytime and prolonged growing seasons elevate carbon sequestration. Therefore, it is difficult to predict the response of ecosystem structure, processes, and functions to global warming when only considering daily mean temperature and daytime temperature. Accordingly, it is necessary to further examine the asymmetric effects of daytime and night-time warming on natural ecosystems.

Generally, the method for assessing the vegetation response to climate changes can be grouped into three categories, which include controlled experiments, model simulations, and quantitative remote sensing surveys. Controlled experiments include the transplantation of undisturbed soil vegetation to plots along different altitude gradients, artificial warming experiments, and soil heating experiments [5–7]. Although controlled experiments can directly reveal the asymmetric effects of warming on vegetation, it is difficult to quantitatively assess such responses at a large scale and across different ecosystems owing to the restriction of manpower and material resources. Model simulation can use quantitative models to simulate the impact of historical warming periods on vegetation and to forecast the influence of future global warming on vegetation [8,9]. However, asymmetric diurnal warming is not currently taken into account by many global carbon cycle models, which affects the accuracy of regional and global models. Quantitative remote sensing methods can quantitatively evaluate large-scale responses of vegetation to T_{\max} and T_{\min} based on time series of remote sensing data [4,10]. Additionally, previous studies have shown that the response of vegetation to changes in T_{\max} and T_{\min} may differ between regions and ecosystem [4,10–14]. Therefore, it is vital to employ a spatially explicit and quantitative tool to assess the effects of daytime and night-time warming to enable better ecosystem management and adaptation.

Satellite-based measurements can provide this type of broad perspective for identifying the spatial heterogeneity of land surface dynamics over the past three decades and to discern the spatiotemporal patterns of vegetation responses to asymmetric diurnal warming [4]. The Normalized Difference Vegetation Index (NDVI), which is related to green leaf biomass and vigor, has proven to be a robust indicator of vegetation growth [15]. The Global Inventory Modeling and Mapping Studies (GIMMS) NDVI dataset, which is the most complete and longest remote sensing dataset, has been used successfully in long-term monitoring studies of vegetation dynamics and climate change impacts on vegetation at regional and global scales [13,16]. Therefore, in order to better understand, simulate, and forecast the response of terrestrial ecosystems to global changes, it is essential that research on the responses of terrestrial vegetation to global warming is based on remote sensing time series data, especially when examining areas that are sensitive to climate change.

As the third pole of the Earth, the Tibetan Plateau, has a unique pattern of natural and hydrothermal spatial differentiation that exhibits gradual change in climate from its warm and humid southeastern regions to its cold and dry northwest. The plateau contains rich, diverse, and fragile vegetation ecosystems and is a natural laboratory for climate change and earth science research [17]. In recent decades, the warming of the Tibetan Plateau has been accompanied by a significant decrease in the diurnal temperature difference, which has been mainly caused by the increase of the minimum temperature in winter and at night. The rate of increase of the land-surface T_{\min} over the past five decades is twice that of T_{\max} [18]. Warming effects on the Tibetan Plateau have a significant impact on both the dynamics of the vegetation during the growing season as well as a profound impact on the plateau's geographical and ecological patterns. Despite an increasing recognition of the critical importance of Tibetan Plateau vegetation for water resource conservation, for biodiversity protection,

for land degradation, and as a carbon source and sink [17], the relationships between vegetation changes and climate warming are not firmly established [19,20].

Additionally, the climate and vegetation across the physico-geographical zone is relatively uniform. Therefore, research on the response of vegetation to climatic elements in different physico-geographical sub-regions can better reveal the characteristics of the regional differences across the plateau. Meanwhile, there are few studies that have compared the different physico-geographical zones to determine the vulnerability of various vegetation types to climate change. Limited efforts have been made to investigate the relative role of daytime and night-time warming in response to different vegetation types. Accordingly, we analyzed how vegetation growth trends have varied across different physico-geographical zones and evaluated the vegetation response to daytime and night-time warming across regions, biomes, and vegetation types.

The objective of this study was to determine the spatiotemporal responses of the terrestrial vegetation on the Tibetan Plateau to daytime and night-time warming. Based on the GIMMS NDVI3g data from 1982 to 2015, we investigated where and to what extent vegetation growth trends on the Tibetan Plateau have been affected by daytime and night-time warming. We also investigated information on the climatic factors, physico-geographical zones, and land cover types. These results could provide insights into the regions of the Tibetan Plateau that are most vulnerable to environmental change and, therefore, support sustainable land management.

2. Materials and Methods

2.1. Data Sources and Processing

NDVI is a sensitive indicator of vegetation productivity, vegetation biomass, and fractional vegetation coverage. It has been widely used to quantify the processes, status, and trends of vegetation growth [21]. This study used the third-generation of NDVI dataset (NDVI3g), which was produced by the GIMMS group based on NOAA/AVHRR series satellites (NOAA-7, 9, 11, 14, 16, and 17). The data at a spatial resolution of $1/12^\circ$ in 15-day time intervals during 1982–2015 were provided by the Ecological Forecasting Lab at the NASA Ames Research Center (<http://ecocast.arc.nasa.gov/>). The dataset has been corrected to reduce noise resulting from sensor degradation, orbital drift, solar zenith angles, volcanic eruptions, sensor shift among the six satellites, and other extraneous factors that have exerted nonlinear and non-stationary effects on the data [19,22]. To further mitigate the contamination of the clouds and the atmospheric turbulence, we obtained the monthly NDVI3g dataset using the Maximum Value Composite (MVC) method. Growing seasonal NDVI (April–October) was defined as the average monthly composite NDVI during the growing season, which has been widely used to assess the photosynthetic activities of vegetation [4,10,23]. In order to minimize the influence of soil variation on spectral signal in bare and sparsely vegetated zones, we only considered the pixels with an average growing-season NDVI greater than 0.1 [13,24].

Based on the time period of GIMMS NDVI3g data, T_{\max} , T_{\min} , precipitation, and solar radiation were collected from 135 meteorological stations across and around the Tibetan Plateau (see Figure 1). These data were provided by the China Meteorological Data Sharing Service System (<http://cdc.cma.gov.cn>). In terms of the geographical coordinates and altitude of each site, these meteorological data except for the solar radiation data were interpolated into a raster dataset at an 8 km resolution by using the thin plate smoothing splines interpolation method, which incorporated topographic effects on spatial climate interpolation [25]. As the solar radiation data were obtained from a few stations, it was difficult to determine reliable patterns of solar radiation using spatial interpolation methods based on ground-based solar radiation observations. Therefore, we used the products of three hourly gridded downward shortwave radiations, which improved the accuracy using estimates by both the surface data-based model and the satellite data [26]. The data were provided by Cold and Arid Regions Science Data Center at Lanzhou, China (<http://westdc.westgis.ac.cn/data>). The maximum and minimum air temperatures during the growing season were calculated as the

average of the daily maximum and minimum air temperature in the same days over years, respectively. The growing season precipitation and radiation were defined as the accumulated precipitation and radiation for the corresponding days, respectively.

The digital elevation model (DEM) data at a 250-m spatial resolution were provided by the NASA Shuttle Radar Topographic Mission (SRTM) website (<http://www.glcf.umd.edu/>; Figure 1). The DEM data were resampled at an 8 km spatial resolution to match the GIMMS NDVI3g data by a cubic spline method. Vegetation distribution information was obtained from a digitized 1:1,000,000 vegetation map of China [27]. The main vegetation type was reclassified as forest, shrubland, cropland, alpine meadow, alpine steppe, and others type (see Figure 1). The vegetation map was resampled to match the spatial resolution of GIMMS NDVI3g data using a majority filter method.

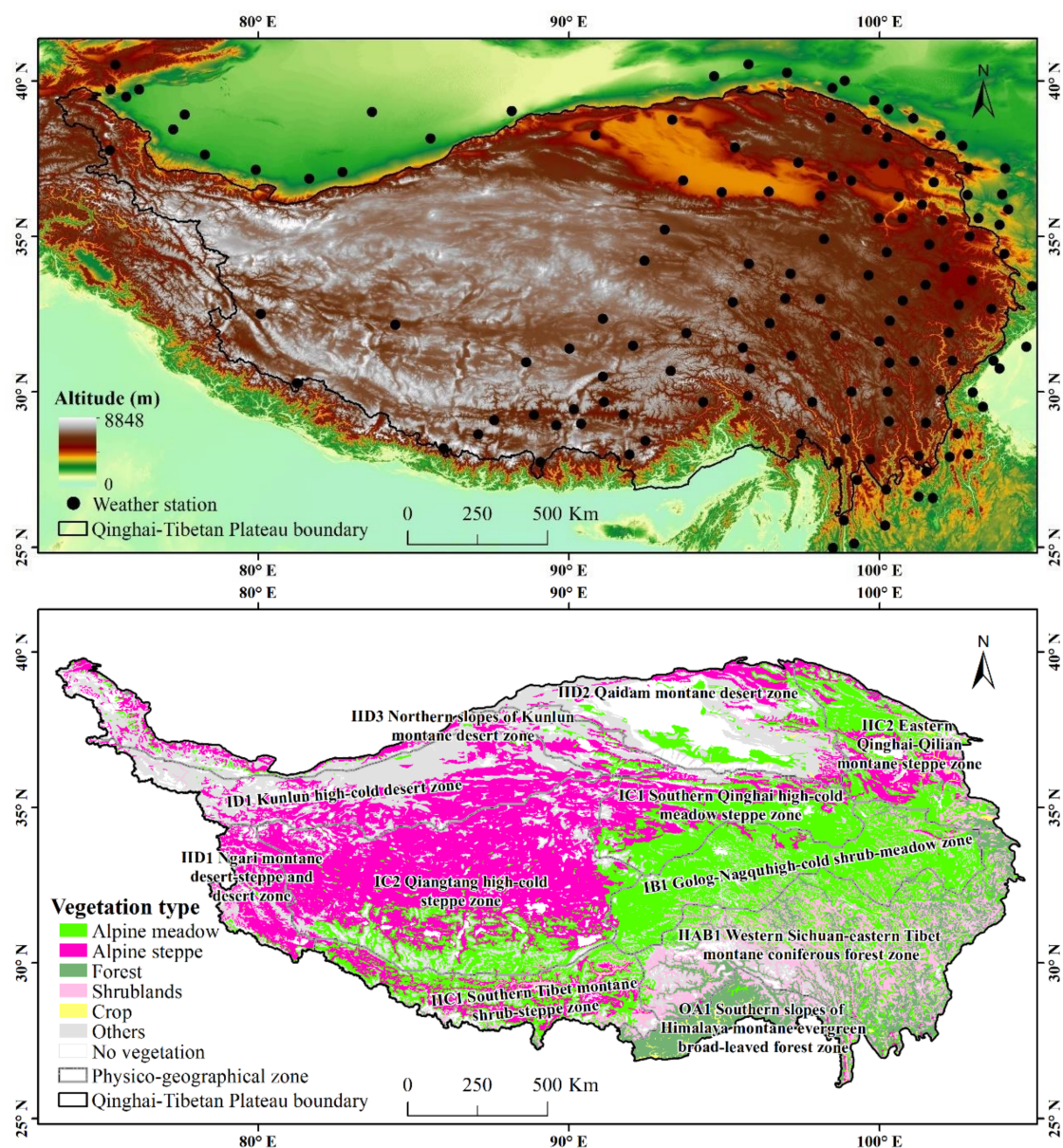


Figure 1. Spatial distribution of the altitude, meteorological stations, vegetation types, and the physico-geographical zones across the Tibetan Plateau.

There are 11 physico-geographical zones of the Tibetan Plateau [28] including IB1 or Golog–Nagqu high-cold shrub-meadow zone, IC1 or Southern Qinghai high-cold meadow

steppe zone, IC2 or Qangtang high-cold steppe zone, ID1 or Kunlun high-cold desert zone, IIAB1 or Western Sichuan-eastern Tibet montane coniferous forest zone, IIC1 or Southern Tibet montane shrub-steppe zone, IIC2 or Eastern Qinghai-Qilian montane steppe zone, IID1 or Ngari montane desert-steppe and desert zone, IID2 or Qaidam montane desert zone, IID3 or Northern slopes of Kunlun montane desert zone, and OA1 or Southern slopes of Himalaya montane evergreen broad-leaved forest zone. In order to reduce error and the uncertainty of the results, we used the same coordinate systems for the GIMMS NDVI3g data, climate data, DEM data, vegetation map, and physico-geographical zone map of the Tibetan Plateau, i.e., World Geodetic System 1984 (WGS84).

2.2. Data Analysis

2.2.1. Linear Regression Trends

In order to analyze the changes of T_{\max} (and T_{\min}) across the Tibetan Plateau, a linear regression was fitted using Equation (1). The statistical significance of the trend called the slope was evaluated based on the correlation coefficient in the regression equation.

$$y = a + bx + e \quad (1)$$

where y denotes the T_{\max} (or T_{\min}) for year x and e is the deviation of the data from the straight line defined by the intercept a and slope b . Positive and negative values of the correlation coefficient b represent increases or decreases, respectively, in T_{\max} (or T_{\min}). The coefficients a and b were determined using least-squares fitting.

2.2.2. Partial Correlation Analysis

Partial correlation analyses were used to detect the relationship between each dependent variable and each particular independent variable by excluding the confounding effects of other variables [4,10,29,30]. The absolute values of each partial correlation coefficient were categorized as greater than or equal to zero and less than or equal to one. When the absolute value of a partial correlation is equal to one, the two variables are completely related. In contrast, when a partial correlation is equal to zero, the two variables are completely unrelated. Since precipitation and solar radiation also influence NDVI [9], variation in precipitation and short solar radiation were taken into account in the partial correlation analysis.

The statistical significance of the partial correlation coefficient between growing season NDVI and T_{\max} (or T_{\min}) after controlling for T_{\min} (or T_{\max}), precipitation, and short solar radiation were evaluated by the Student's t -test as seen in Equation (2).

$$t = r \left[(n - q - 1) / (1 + r^2) \right]^{1/2} \quad (2)$$

where n , q , and r are the total number of years, the number of independent variables, and the partial correlation coefficient between growing-season NDVI and T_{\max} (or T_{\min}) after controlling for T_{\min} (or T_{\max}), precipitation, and short solar radiation.

3. Results

3.1. Trends of Daytime and Night-Time Warming in Tibetan Plateau

The increasing trend in T_{\min} over the past three decades is 1.7 times that in T_{\max} over the Tibetan Plateau during the growing season (see Figure A1). From 1982 to 2015, the warming trend of T_{\max} and T_{\min} has occurred over 94.2% and 99.8% of the total study area, respectively (Figure 2a,b). Additionally, T_{\max} and T_{\min} show statistically significant warming across 68.1% ($p < 0.05$) and 95.9% ($p < 0.05$) of the Tibetan Plateau, respectively. T_{\max} in the northwest and south of the Tibetan Plateau showed a statistically significant downward trend and the declining area occupied only 5.8% of the study area.

Additionally, the warming trend and increasing amplitude for T_{\max} and T_{\min} were not consistent across the Tibetan Plateau. Figure 2c shows the difference between T_{\max} and T_{\min} (DTR) on the Tibetan Plateau during 1982–2015. The trend in DTR is heterogeneous across the Tibetan Plateau. DTR decreased in 69.8% of the Tibetan Plateau particularly in the Midwest portion of the plateau (see Figure 2c) of which 43.5% was statistically significant ($p < 0.05$). In contrast, DTR increased over about 30.2% of the total study area of which 10.6% was statistically significant ($p < 0.05$).

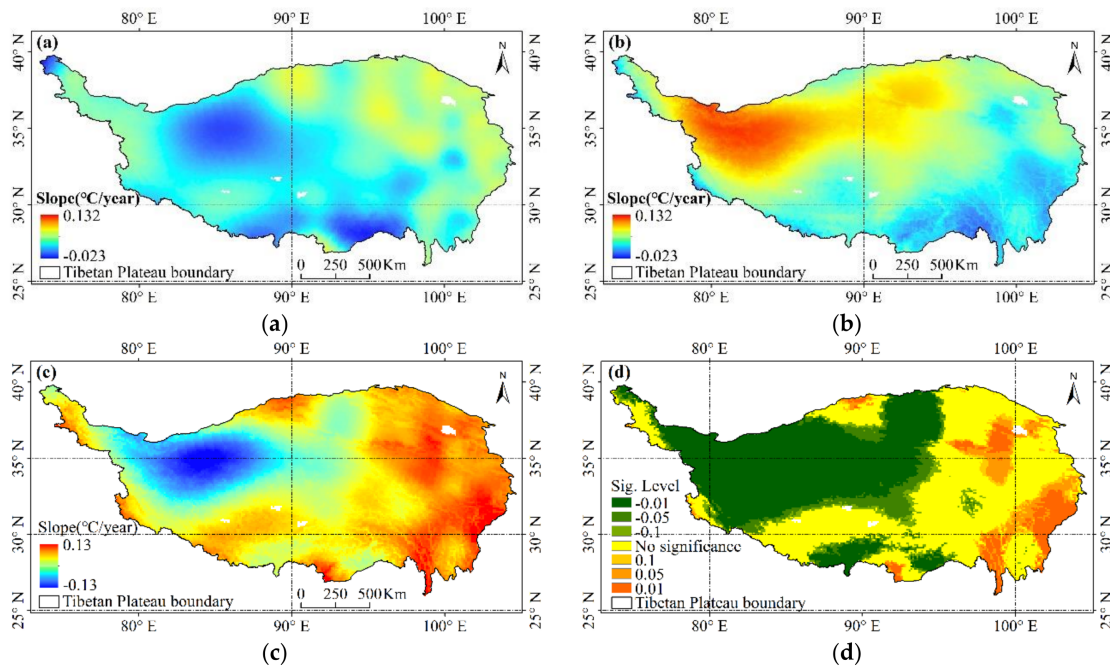


Figure 2. Air temperature trends in the Tibetan Plateau from 1982 to 2015. (a) The slope of T_{\max} ; (b) the slope of T_{\min} ; (c) the slope of DTR; and (d) the significance level of DTR trends.

3.2. Partial Correlations between NDVI and Diurnal Extreme Temperature on the Tibetan Plateau

When the effects of growing season T_{\min} , precipitation, and solar radiation were removed from the partial correlation, the individual effect of growing season T_{\max} inter-annual changes on inter-annual NDVI was obtained, which revealed a remarkable spatial pattern (see Figure 3a). Overall, 74.4% of the area exhibited a positive correlation between NDVI and T_{\max} and 18.5% of the region showed a significantly positive correlation ($p < 0.05$; Figure 3a). These significant positive correlations between NDVI and T_{\max} were found mainly within the wetter or colder regions including IB1, IC1, IIC2, OA1, and the western portion of IIAB1 (see Figure 3a). In addition, 25.6% of the area exhibited a negative correlation between NDVI and T_{\max} with 1.1% of the total region showing a statistically significant negative correlation between these variables ($p < 0.05$). The negative correlations between NDVI and T_{\max} occurred across the semi-arid and arid region including IIC1, IID3, IID2, and the western portion of IC2.

While the effects of growing-season T_{\max} , precipitation, and solar radiation were removed in the partial correlation analysis, the individual effect of growing season T_{\min} interannual changes on interannual NDVI was also obtained (see Figure 3b). While 46.6% of the region exhibited positive correlations between NDVI and T_{\min} during the growing season, 7.8% of the total area exhibited significant positive correlations ($p < 0.05$; Figure 3b). These statistically significant positive correlations between NDVI and T_{\min} were found mainly in the high-cold steppe and meadow steppe zones (i.e., IC1, IIC1, IC2, IID3, and ID1). In contrast, 53.4% of the region showed negative correlations between NDVI and T_{\min} during the growing season with 8.3% of the total area exhibiting a significant

negative correlation ($p < 0.05$). The negative correlations between NDVI and T_{\min} exhibit a more complex pattern and occur in the montane steppe zone (i.e., IID2) and wet forest (i.e., OA1) regions.

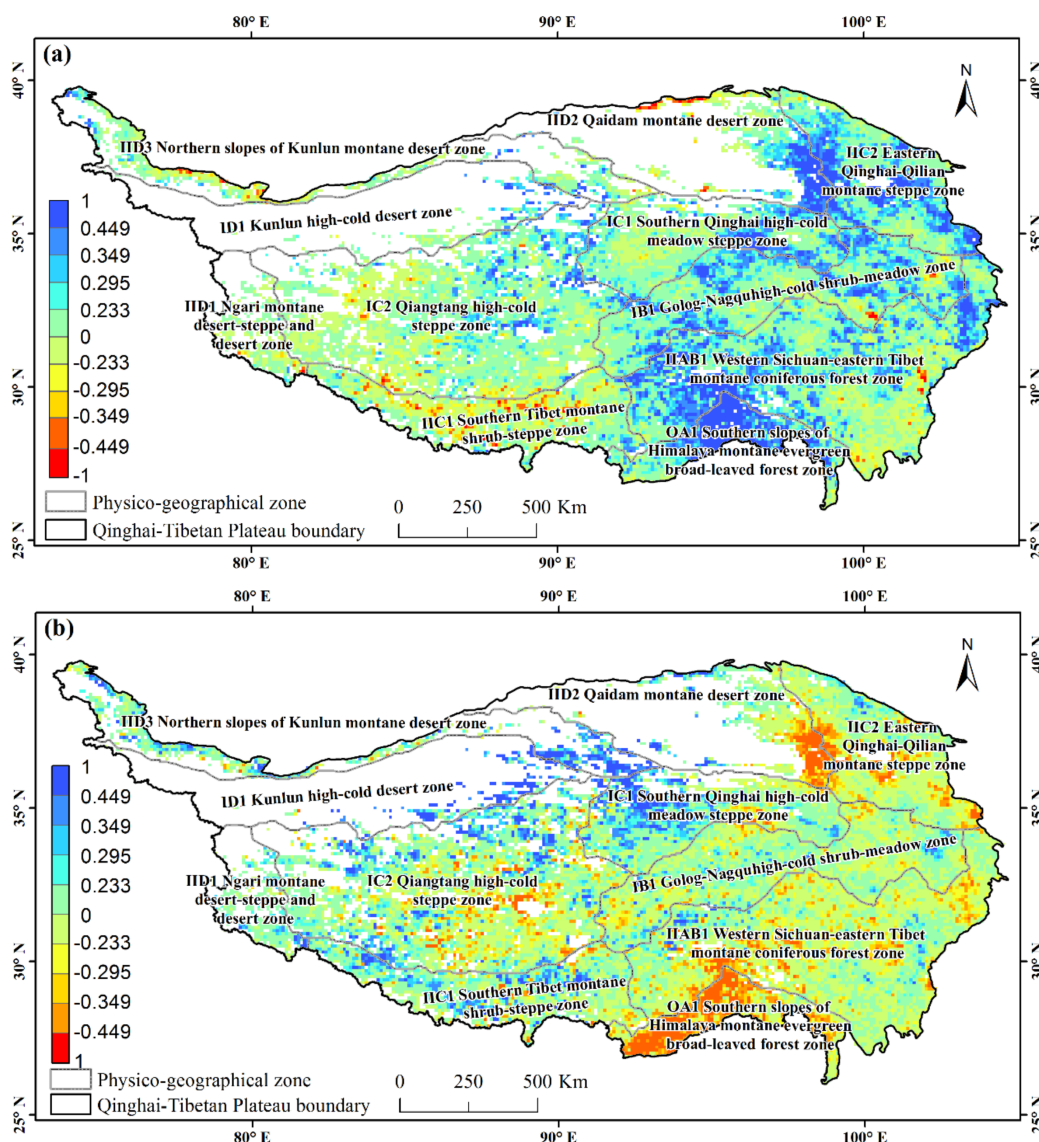


Figure 3. Spatial patterns of the correlations between growing season (April–October) NDVI and corresponding daily maximum (T_{\max}) or minimum temperatures (T_{\min}) in the Tibetan Plateau during 1982–2015. (a) The spatial patterns of partial correlation coefficients between NDVI and T_{\max} . The corresponding T_{\min} , precipitation, and solar radiation are controlled for in the calculation. (b) The partial correlation coefficients between NDVI and T_{\min} during the growing season with T_{\max} , precipitation, and solar radiation controlled for. The color-coded values ± 0.449 , ± 0.349 , ± 0.295 , and ± 0.233 correspond to p -values of 0.01, 0.05, 0.10, and 0.20 according to two-tailed Student's t -tests.

3.3. Partial Correlations between NDVI and Asymmetric Diurnal Warming in Different Physico-Geographical Regions

Dynamic changes in vegetation were closely related to changes in T_{\max} and T_{\min} simultaneously. The unique topography and location of the Tibetan Plateau forms a unique alpine plateau climate. The synergistic effect of T_{\max} or T_{\min} on the alpine vegetation can be categorized into four types (see Figure 4). The first type includes the partial correlation coefficient between NDVI of the alpine vegetation and T_{\max} or T_{\min} , which were both positive with 25.7% of the plateau area were in

this category. The percentage of the area for each physico-geographical zone meeting the criteria was the highest in IC1 (48.3%), followed by IB1 (35.3%), IC2 (25.1%), IIC2 (22.7%), IIAB1 (17.2%), IIC1 (12.7%), and OA1 (2.8%) in descending order. These were high-cold steppe or meadow zones in which vegetation growth is mainly limited by heat. Therefore, increases in T_{max} and T_{min} both accelerate the growth of vegetation. The second type includes the correlations between the NDVI of the alpine vegetation and T_{max} or T_{min} were both negative. This category occupies only 4.7% of the plateau, which is ranked at the lowest of the four categories by area. The physico-geographical zone that was most comprised of this category of area was IIC1 (9.6%), followed by IC2 (6.7%), IIAB1 (6.6%), OA1 (6.3%), IB1 (2.5%), IIC2 (1.3%), and IC1 (0.6%) in descending order. In other words, there were few areas where the night and day warming have each had effects on the vegetation of the Tibetan Plateau. The third type includes the correlation coefficient between the NDVI of the alpine vegetation and the T_{max} or T_{min} values, which were positive and negative, respectively. A total of 48.7% of the plateau area was in this category, which was the largest among the four categories. The physico-geographical zone that was most comprised of this category of area corresponding to this category was OA1 (90.3%), followed by IIC2 (69.6%), IIAB1 (62.2%), IB1 (50.2%), IC2 (40.3%), IC1 (30.9%), and IIC1 (29.3%) in descending order. In general, daytime warming has had a positive impact on most of the vegetation and nighttime warming enhanced carbon consumption which has had a negative impact on the vegetation NDVI on the Tibetan Plateau. In the last category, the correlation coefficient between the NDVI of the alpine vegetation and the T_{max} and T_{min} values were negative and positive, respectively, with 20.9% of the plateau area in this category. The physico-geographical zone comprised the largest part of this category was IIC1 (48.4%), followed by IC2 (27.9%), IC1 (20.1%), IIAB1 (14.0%), IB1 (12.0%), IIC2 (6.5%), and OA1 (0.6%) in descending order. In these areas, vegetation grew more during the day when the maximum temperature dropped and the nighttime minimum temperature increased. As ID1, IID1, IID2, and IID3 were desert zones, the NDVI in most of these regions was lower than 0.1. Therefore, these four regions were not analyzed in this particular analysis.

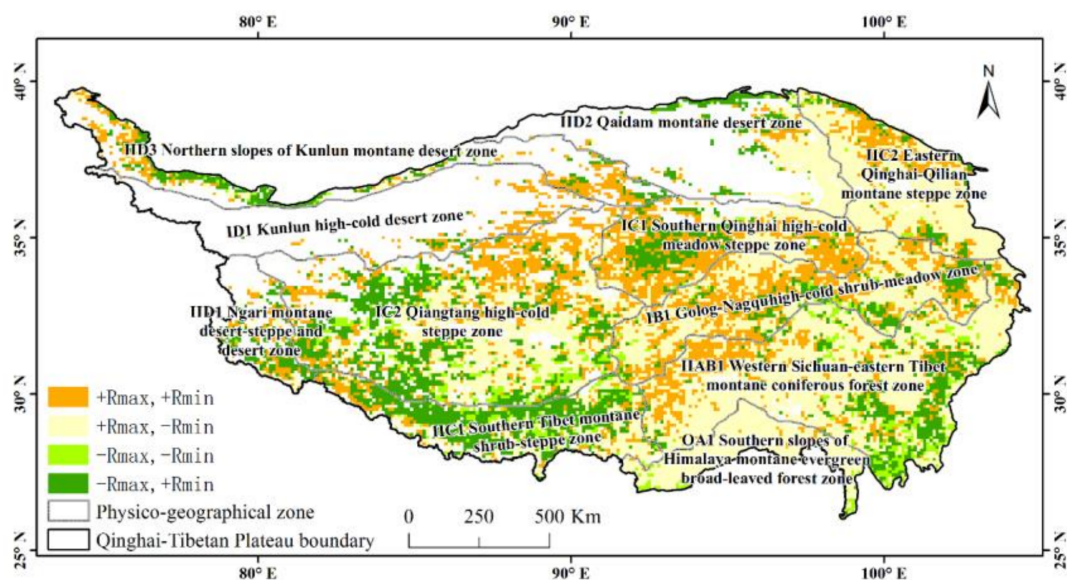


Figure 4. Spatial patterns of the correlation between NDVI in growing season (April–October) and corresponding daily maximum (T_{max}) or minimum temperatures (T_{min}) of the Tibetan Plateau from 1982–2015. R_{max} represents the spatial patterns of partial correlation coefficients between NDVI and T_{max} . The corresponding T_{min} , precipitation, and solar radiation were controlled for in the calculation. R_{min} shows the partial correlation coefficients between NDVI and T_{min} during the growing season with T_{max} , precipitation, and solar radiation are controlled for. + denotes positive partial correlations while – denotes negative partial correlations.

3.4. Partial Correlations between NDVI and Asymmetric Diurnal Warming among Different Vegetation Types

In order to assess correlations between NDVI and diurnal warming during the growing season for various vegetation types, we analyzed the correlation between NDVI and T_{max} (or T_{min}) in the growing season after eliminating the effects of T_{min} (or T_{max}), precipitation, and solar radiation (see Table 1). Partial correlations between growing season NDVI and T_{max} were positively correlated with forest and crop vegetation areas exhibiting high significance ($p < 0.01$) while shrubland and others type were also significantly correlated ($p < 0.05$) with T_{max} and alpine meadow appearing marginally significant ($p < 0.1$). However, partial correlations between the growing season NDVI and T_{min} exhibited obvious divergence among the different vegetation types with all but alpine steppes and other types of vegetation that exhibit negative correlations. Forest ($p < 0.01$), crop ($p < 0.05$), and shrublands ($p < 0.1$) showed statistical significance in these correlations. Generally speaking, daytime warming enhanced vegetation growth while night-time warming had a positive impact on alpine steppe vegetation and the other types. In contrast, night-time warming had an adverse effect on forest, shrublands, alpine meadow, and crop vegetation types.

Table 1. Partial correlation coefficients between NDVI and T_{max} and T_{min} for different vegetation types.

Vegetation Type	T_{max}	T_{min}
Forest	0.598 ***	−0.561 ***
Shrublands	0.446 **	−0.337 *
Alpine Steppe	0.132	0.263
Alpine Meadow	0.301 *	−0.39
Crop	0.455 ***	−0.428 **
Others	0.407 **	0.125

Note: *** $p < 0.01$, ** $p < 0.05$, * $p < 0.1$ (two-tailed).

To assess the spatial patterns of the responses of different vegetation types to daytime and night-time warming, we compared percentages of statistically significant (i.e., $p < 0.05$) pixels among each of the different vegetation types (see Table 2). The partial correlation coefficient between NDVI and T_{max} relative to that between NDVI and T_{min} for all vegetation types was more significant including the higher proportion of crop (41.46%), forest (34.64%), shrublands (23.04%), and alpine meadow (18.68%). In contrast, the percentage of pixels with significant partial correlations between NDVI and T_{min} were generally relatively low for all vegetation types except for alpine steppe (19.86%) and others type (20.49%). The positive partial correlation between NDVI and T_{max} exhibited overwhelming majority, but for partial correlation between NDVI and T_{min} , forest (25.73%), shrublands (10.94%), and crop (39.02%) mainly showed negative correlations. Alpine steppe (14.01%), alpine meadow (5.92%), and others type (12.25%) mainly exhibited positive correlations. Taken together, the response of vegetation to daytime and night-time warming varied across vegetation types (Tables 1 and 2). We found that daytime warming has significantly positive influence on all types of vegetation while night-time warming has significantly negative influences on forest, shrublands, and crop vegetation types and has statistically significant positive influence on alpine steppe, alpine meadow, and other types of vegetation.

Table 2. Percentages of statistically significant ($p < 0.05$) pixels among vegetation types (%).

Vegetation Types	T_{\max}			T_{\min}		
	+	−	Total	+	−	Total
Forest	34.22	0.42	34.64	0.31	25.73	26.04
Shrublands	22.18	0.86	23.04	1.97	8.97	10.94
Alpine Steppe	11.06	1.62	12.68	14.01	5.83	19.86
Alpine Meadow	17.81	0.87	18.68	5.92	4.08	10.00
Crop	41.46	0	41.46	0	39.02	39.02
Others	17.75	1.04	18.79	12.25	8.24	20.49

4. Discussion

We found that annual T_{\max} and T_{\min} of the Tibetan Plateau increased significantly from 1982 to 2015 and the spatial patterns of warming were heterogeneous. The increasing rate of seasonal T_{\min} over the past three decades was 1.7 times that of seasonal T_{\max} . This result suggested that the asymmetric diurnal warming existed in Tibetan Plateau, which was consistent with previous studies. For example, Liu and Chen (2000) found that the majority of the Tibetan Plateau has experienced statistically significant warming since the mid-1950s [31]. Jun et al. (2013) suggested that there has been significant warming in T_{\max} and T_{\min} over the past three decades, especially for T_{\min} [32]. Ma and Li (2003) demonstrated that the annual increases in T_{\min} over the past three decades have been one to three times that of T_{\max} across weather stations [33].

Vegetation NDVI of the Tibetan Plateau was predominantly positively correlated with changes in T_{\max} and 18.5% of the region showed significantly positive correlations ($p < 0.05$). These statistically significant positive correlations between NDVI and T_{\max} were found mainly in the colder or wetter regions which were IB1, IC1, IIC2, the west parts of IIAB1, and OA1. Peng et al. (2013) found that growing season NDVI was positively correlated with growing season T_{\max} in Tibetan Plateau [4]. Liang et al. (2015) found that NDVI showed a significantly positive partial correlation with T_{\max} in the wetland vegetation of Nansi Lake [34]. In the high-cold humid mountain regions, photosynthetic activity of the vegetation is limited by temperature more than water [13,35]. Therefore, the photosynthetic enzyme activity is generally enhanced as T_{\max} rises [36]. In contrast, in drier steppe regions (IIC1, IID1, IID2, IID3, and the western portion of IC2), interannual T_{\max} anomalies exhibit negative partial correlations with NDVI. Peng et al. (2013) also suggested that such negative correlations between NDVI and T_{\max} would occur in drier temperate regions [4]. This negative correlation between T_{\max} and NDVI could be related to increased water stress via warming-induced soil moisture depletion [23,37]. Moreover, decreased vegetation NDVI can reduce latent heat and increase sensible heat, which can result in additional warming [38]. Previous field experiments also observed that the soil moisture in root zone significantly changed with warming temperature, which negatively affects vegetation photosynthetic activity [39,40].

However, in arid and semi-arid regions, we found that vegetation NDVI exhibited statistically significant positive correlations ($p < 0.05$) between NDVI and growing season T_{\min} while the T_{\max} , precipitation, and solar radiation were controlled for. Additionally, in the wettest forest and coldest montane steppe zone, vegetation NDVI presenting statistically significant negative correlations ($p < 0.05$) between NDVI and growing season T_{\min} after the T_{\max} , precipitation, and solar radiation were controlled for. These opposite responses of NDVI to T_{\min} between the wet and dry regions of the Tibetan Plateau could be attributed to night-time warming enhancing vegetation respiration, which leads to the consumption of more material and energy. As a result, it stimulates photosynthesis of vegetation the next day. Therefore, improving vegetation transpiration is accompanied by helping atmospheric CO_2 enter the leaves for photosynthesis, which enhances vegetation growth as indicated by NDVI. For instance, Wan et al. (2009) suggested that an increase in T_{\min} will enhance growth at a temperate, dry grassland site in China [41]. However, Peng et al. (2004) demonstrated that an increase in T_{\min} will reduce rice yields by 10% per degree Celsius in the Philippines [12]. Peng et al.

(2013) also observed these opposite responses of NDVI to T_{\min} between the wet and dry regions of the Northern Hemisphere [4]. The reasons for this contrasting behavior may be related to the different mechanisms of temperature change across the plateau vegetation. Wang and Zhou (2004) studied the response characteristics of *Leymus chinensis* steppe in Inner Mongolia to temperature changes by using multi-year observational data from given plots and found that the response characteristics of different plant species to winter T_{\min} changes differed [42]. Both this study and the previous research [4,12,41] showed that there were differences in the characteristics of diurnal warming which affected vegetation activities, and that the responses of different ecosystem types also differ. Additional detail research that integrates physiological, ecological, and hydrological observations would assist to better understand and explain the unique climate on the Tibetan Plateau.

In addition, we found that vegetation NDVI in different undisturbed natural areas of the Tibetan Plateau have had different responses to diurnal warming. The combination of altitudes, latitudes, and longitudes across the Tibetan Plateau forms hydrothermal patterns and alpine resources and environments, which lead to differences in the response of the same vegetation types to diurnal warming. The phenomenon of compensation is ubiquitous among life forms affected by stress and injuries and it is considered an adaptation of organisms to adverse environments [43]. Therefore, the compensatory physiological responses of individual plants may also promote the different responses on broader scales and among the same vegetation to diurnal warming.

The temporal and spatial change in vegetation NDVI was the result of a combination of natural and anthropogenic factors. Certainly, it should be noted that grassland NDVI is also regulated by grassland degradation [44], thawing–freezing processes [45], and declining snow cover [46]. In this study, the correlation between diurnal temperature and vegetation NDVI change was analyzed. Anthropogenic factors were not taken into account.

5. Conclusions

Our results suggested that the Tibetan Plateau has experienced a warming trend and the increasing rate of T_{\min} over the past three decades was much higher than T_{\max} . The warming trend and magnitude of T_{\min} and T_{\max} have not been uniform across the Tibetan Plateau. After removing the correlation between T_{\max} and T_{\min} , the partial correlation between T_{\max} and NDVI was significantly positive in wetter and colder regions of the Tibetan Plateau, but negative in the semi-arid southwest of the Tibetan Plateau. In contrast, the partial correlation between T_{\min} and NDVI is positive in the high-cold steppe and meadow steppe zones and exhibits a significant negative behavior in the montane steppe zone and wet forest zone. Meanwhile, asymmetric diurnal warming in the Tibetan Plateau has different effects on different types of vegetation. Daytime warming has significantly positive influences on all the vegetation, while night-time warming has mainly significantly negative influences on forest, shrublands, and crop vegetation types and has statistically significant positive influences on alpine steppe, alpine meadow, and others type.

The results of this study suggested that the variation in vegetation responses to diurnal temperature changes is important for understanding the changes in vegetation photosynthetic activity in a warming world. As future climate data shows the potential for asymmetric warming in global land surface climates, our results provide a reference for assessing and predicting vegetation responses to global climate change. Future research is needed to integrate T_{\max} and T_{\min} using remote sensing-based ecosystem models to reduce uncertainty regarding the terrestrial carbon cycle and corresponding climate feedback effects.

Acknowledgments: This research was funded jointly by the National Natural Science Foundation project of China (41631180, 41671536, 41571373, 41701503, and 41701433), the National Key Research and Development Program of China (No. 2016YFA0600103, 2016YFC0500201-06), and the program for key scientific research in the University of Henan Province (18A170002). We are grateful to all contractors, image providers, and the anonymous reviewers for their valuable comments and suggestions.

Author Contributions: Haoming Xia and Yaochen Qin. conceived and designed the experiments. Haoming Xia performed programming work, analysis, discussions, and wrote most sections of the manuscript. Ainong Li, Gary Feng, Yang Li, Yaochen Qin, Guangbin Lei, and Yaoping Cui supplied suggestions and comments for the manuscript. All authors reviewed and adjusted the manuscript.

Conflicts of Interest: The authors declare no conflict of interest.

Appendix

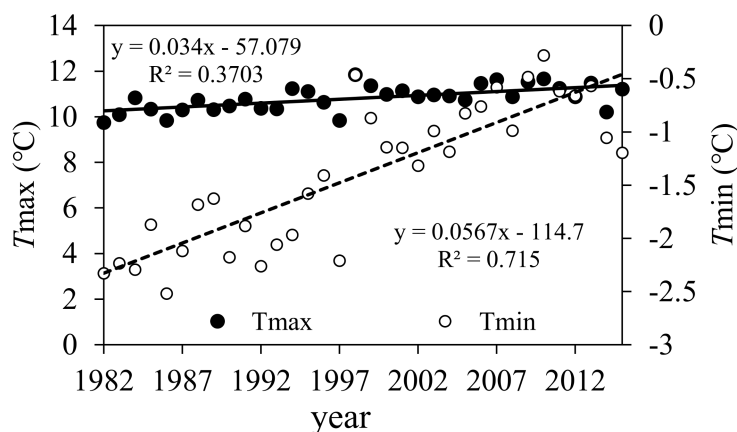


Figure A1. Variations in T_{\max} and T_{\min} during growing seasons on Tibetan Plateau from 1982 to 2015.

References

1. Parmesan, C.; Yohe, G. A globally coherent fingerprint of climate change impacts across natural systems. *Nature* **2003**, *421*, 37–42. [[CrossRef](#)] [[PubMed](#)]
2. Intergovernmental Panel on Climate Change (IPCC). *Climate Change 2013: The Physical Science Basis. Contribution of Working Group I to the Fifth Assessment Report of the Intergovernmental Panel on Climate Change*; Cambridge University Press: Cambridge, UK; New York, NY, USA, 2013.
3. Screen, J.A. Arctic amplification decreases temperature variance in northern mid- to high-latitudes. *Nat. Clim. Chang.* **2014**, *4*, 577–582. [[CrossRef](#)]
4. Peng, S.; Piao, S.; Ciais, P.; Myneni, R.B.; Chen, A.; Chevallier, F.; Dolman, A.J.; Janssens, I.A.; Peñuelas, J.; Zhang, G. Asymmetric effects of daytime and night-time warming on Northern Hemisphere vegetation. *Nature* **2013**, *501*, 88–94. [[CrossRef](#)] [[PubMed](#)]
5. Frey, S.D.; Drijber, R.; Smith, H.; Melillo, J. Microbial biomass, functional capacity, and community structure after 12 years of soil warming. *Soil Biol. Biochem.* **2008**, *40*, 2904–2907. [[CrossRef](#)]
6. Walker, M.D.; Wahren, C.H.; Hollister, R.D.; Henry, G.H.; Ahlquist, L.E.; Alatalo, J.M.; Bret-Harte, M.S.; Calef, M.P.; Callaghan, T.V.; Carroll, A.B. Plant community responses to experimental warming across the tundra biome. *Proc. Natl. Acad. Sci. USA* **2006**, *103*, 1342–1346. [[CrossRef](#)] [[PubMed](#)]
7. Ma, X.-X.; Yan, Y.; Hong, J.-T.; Lu, X.-Y.; Wang, X.-D. Impacts of warming on root biomass allocation in alpine steppe on the north Tibetan Plateau. *J. Mt. Sci.* **2017**, *14*, 1615–1623. [[CrossRef](#)]
8. Zhang, G.; Kang, Y.; Han, G.; Sakurai, K. Effect of climate change over the past half century on the distribution, extent and NPP of ecosystems of Inner Mongolia. *Glob. Chang. Biol.* **2015**, *17*, 377–389. [[CrossRef](#)]
9. Nemani, R.R.; Keeling, C.D.; Hashimoto, H.; Jolly, W.M.; Piper, S.C.; Tucker, C.J.; Myneni, R.B.; Running, S.W. Climate-driven increases in global terrestrial net primary production from 1982 to 1999. *Science* **2003**, *300*, 1560–1563. [[CrossRef](#)] [[PubMed](#)]
10. Tan, J.; Piao, S.; Chen, A.; Zeng, Z.; Ciais, P.; Janssens, I.A.; Mao, J.; Myneni, R.B.; Peng, S.; Peñuelas, J. Seasonally different response of photosynthetic activity to daytime and night-time warming in the Northern Hemisphere. *Glob. Chang. Biol.* **2015**, *21*, 377–387. [[CrossRef](#)] [[PubMed](#)]
11. Alward, R.D.; Detling, J.K.; Milchunas, D.G. Grassland vegetation changes and nocturnal global warming. *Science* **1999**, *283*, 229–231. [[CrossRef](#)] [[PubMed](#)]

12. Peng, S.; Huang, J.; Sheehy, J.E.; Laza, R.C.; Visperas, R.M.; Zhong, X.; Centeno, G.S.; Khush, G.S.; Cassman, K.G. Rice yields decline with higher night temperature from global warming. *Proc. Natl. Acad. Sci. USA* **2004**, *101*, 9971–9975. [[CrossRef](#)] [[PubMed](#)]
13. Zhou, L.; Tucker, C.J.; Kaufmann, R.K.; Slayback, D.; Shabanov, N.V.; Myneni, R.B. Variations in northern vegetation activity inferred from satellite data of vegetation index during 1981 to 1999. *J. Geophys. Res. Atmos.* **2001**, *106*, 20069–20083. [[CrossRef](#)]
14. Pvv, P.; Pisipati, S.R.; Ristic, Z.; Bukovnik, U.; Fritz, A.K. Impact of Nighttime Temperature on Physiology and Growth of Spring Wheat. *Crop Sci.* **2008**, *48*, 2372–2380.
15. Tucker, C.J. Red and photographic infrared linear combinations for monitoring vegetation. *Remote Sens. Environ.* **1979**, *8*, 127–150. [[CrossRef](#)]
16. Myneni, R.B.; Keeling, C.D.; Tucker, C.J.; Asrar, G.; Nemani, R.R. Increased plant growth in the northern high latitudes from 1981 to 1991. *Nature* **1997**, *386*, 698–702. [[CrossRef](#)]
17. Sun, H.; Du, Z.; Yao, T.; Zhang, Y. Protection and Construction of the National Ecological Security Shelter Zone on Tibetan Plateau. *Acta Ecol. Sin.* **2012**, *67*, 3–12.
18. Duan, A.; Wu, G.; Zhang, Q.; Liu, Q. The warming of the Qinghai-Tibet Plateau is new evidence of the intensification of greenhouse gas emissions. *Chin. Sci. Bull.* **2006**, *51*, 989–992. [[CrossRef](#)]
19. Xu, H.J.; Wang, X.P.; Yang, T.B. Trend shifts in satellite-derived vegetation growth in Central Eurasia, 1982–2013. *Sci. Total Environ.* **2017**, *579*, 1658–1674. [[CrossRef](#)] [[PubMed](#)]
20. Piao, S.; Wang, X.; Ciais, P.; Zhu, B.; Wang, T.; Liu, J. Changes in satellite-derived vegetation growth trend in temperate and boreal Eurasia from 1982 to 2006. *Glob. Chang. Biol.* **2011**, *17*, 3228–3239. [[CrossRef](#)]
21. Buitenwerf, R.; Rose, L.; Higgins, S.I. Three decades of multi-dimensional change in global leaf phenology. *Nat. Clim. Chang.* **2015**, *5*, 364–368. [[CrossRef](#)]
22. Pinzon, J.; Tucker, C. A Non-Stationary 1981–2012 AVHRR NDVI3g Time Series. *Remote Sens. (Basel)* **2014**, *6*, 6929–6960. [[CrossRef](#)]
23. Xu, L.; Myneni, R.; Chapin, F., III; Callaghan, T.; Pinzon, J.; Tucker, C.; Zhu, Z.; Bi, J.; Ciais, P.; Tømmervik, H.; et al. Diminished temperature and vegetation seasonality over northern high latitudes. *Nat. Clim. Chang.* **2013**, 1–7. [[CrossRef](#)]
24. Piao, S.; Cui, M.; Chen, A.; Wang, X.; Ciais, P.; Liu, J.; Tang, Y. Altitude and temperature dependence of change in the spring vegetation green-up date from 1982 to 2006 in the Qinghai-Xizang Plateau. *Agric. For. Meteorol.* **2011**, *151*, 1599–1608. [[CrossRef](#)]
25. Hutchinson, M.F. Interpolating mean rainfall using thin plate smoothing splines. *Int. J. Geogr. Inf. Sci.* **1995**, *9*, 385–403. [[CrossRef](#)]
26. Yang, K.; Jie, H.; Tang, W.; Qin, J.; Cheng, C.C.K. On downward shortwave and longwave radiations over high altitude regions: Observation and modeling in the Tibetan Plateau. *Agric. For. Meteorol.* **2010**, *150*, 38–46. [[CrossRef](#)]
27. Chinese Academy of Sciences. *Vegetation Atlas of China*; Science Press: Beijing, China, 2001.
28. Zhang, Y.; Qi, W.; Zhou, C.; Ding, M.; Liu, L.; Gao, J.; Bai, W.; Wang, Z.; Zheng, D. Spatial and temporal variability in the net primary production (NPP) of alpine grassland on Tibetan Plateau from 1982 to 2009. *Acta Ecol. Sin.* **2013**, *24*, 1197–1211.
29. Beer, C.; Reichstein, M.; Tomelleri, E.; Ciais, P.; Jung, M.; Carvalhais, N.; Rödenbeck, C.; Arain, M.A.; Baldocchi, D.; Bonan, G.B. Terrestrial gross carbon dioxide uptake: Global distribution and covariation with climate. *Science* **2010**, *329*, 834–838. [[CrossRef](#)] [[PubMed](#)]
30. Yu, H.; Luedeling, E.; Xu, J. Winter and spring warming result in delayed spring phenology on the Tibetan Plateau. *Proc. Natl. Acad. Sci. USA* **2010**, *107*, 22151–22156. [[CrossRef](#)] [[PubMed](#)]
31. Liu, X.; Chen, B. Climatic warming in the Tibetan Plateau during recent decades. *Int. J. Climatol.* **2000**, *20*, 1729–1742. [[CrossRef](#)]
32. Jun, D.U.; Hongya, L.U.; Jian, J. Variations of extreme air temperature events over Tibet from 1961 to 2010. *Acta Ecol. Sin.* **2013**, *68*, 1269–1280.
33. Ma, X.; Li, D. Analyses on air temperature and its abrupt change over Qinghai-Xizang Plateau in Modern age. *Plateau Meteorol.* **2003**, *22*, 507–512.
34. Liang, C.; Yu, Q.; Liu, Y.; Zhang, Z. Effects of air temperature circadian on the NDVI of Nansi lake wetland vegetation. *Trop. Geogr.* **2015**, *35*, 422–426.

35. Lucht, W.; Prentice, I.C.; Myneni, R.B.; Sitch, S.; Friedlingstein, P.; Cramer, W.; Bousquet, P.; Buermann, W.; Smith, B. Climatic control of the high-latitude vegetation greening trend and Pinatubo effect. *Science* **2002**, *296*, 1687–1689. [[CrossRef](#)] [[PubMed](#)]
36. Turnbull, M.H.; Murthy, R.; Griffin, K.L. The relative impacts of daytime and night-time warming on photosynthetic capacity in *Populus deltoides*. *Plant Cell Environ.* **2002**, *25*, 1729–1737. [[CrossRef](#)]
37. Vicenteserrano, S.M.; Gouveia, C.; Camarero, J.J.; Beguería, S.; Trigo, R.; Lópezmoreno, J.I.; Azorínmolina, C.; Pasho, E.; Lorenzolacruz, J.; Revuelto, J. Response of vegetation to drought time-scales across global land biomes. *Proc. Natl. Acad. Sci. USA* **2013**, *110*, 52–57. [[CrossRef](#)] [[PubMed](#)]
38. Jeong, S.J.; Ho, C.H.; Kim, K.Y.; Jeong, J.H. Reduction of spring warming over East Asia associated with vegetation feedback. *Geophys. Res. Lett.* **2009**, *36*, 1–5. [[CrossRef](#)]
39. Adams, H.D.; Guardiolaclaramonte, M.; Barrongafford, G.A.; Villegas, J.C.; Breshears, D.D.; Zou, C.B.; Troch, P.A.; Huxman, T.E. Temperature sensitivity of drought-induced tree mortality portends increased regional die-off under global-change-type drought. *Proc. Natl. Acad. Sci. USA* **2009**, *106*, 7063–7066. [[CrossRef](#)] [[PubMed](#)]
40. Llorens, L.; Penuelas, J.; Filella, I. Diurnal and seasonal variations in the photosynthetic performance and water relations of two co-occurring Mediterranean shrubs, *Erica multiflora* and *Globularia alypum*. *Physiol. Plant.* **2003**, *118*, 84–95. [[CrossRef](#)] [[PubMed](#)]
41. Wan, S.; Xia, J.; Liu, W.; Niu, S. Photosynthetic Overcompensation under Nocturnal Warming Enhances Grassland Carbon Sequestration. *Ecology* **2009**, *90*, 2700–2710. [[CrossRef](#)] [[PubMed](#)]
42. Wang, Y.; Zhou, G. Response of *Leymus Chinensis* Grassland Vegetation in Inner Mongolia to Temperature change. *Acta Phytoecol. Sin.* **2004**, *28*, 507–514.
43. Hu, T.; Kang, S. The compensatory effect in drought resistance of plants and its application in water-saving agriculture. *Acta Ecol. Sin.* **2005**, *25*, 885–891.
44. Hu, H.C.; Wang, G.X.; Liu, G.S.; Li, T.B.; Ren, D.X.; Wang, Y.; Cheng, H.Y.; Wang, J.F. Influences of alpine ecosystem degradation on soil temperature in the freezing-thawing process on Qinghai-Tibet Plateau. *Environ. Geol.* **2009**, *57*, 1391–1397. [[CrossRef](#)]
45. Yang, M.; Yao, T.; Gou, X.; Koike, T.; He, Y. The soil moisture distribution, thawing–freezing processes and their effects on the seasonal transition on the Qinghai–Xizang (Tibetan) plateau. *J. Asian Earth Sci.* **2003**, *21*, 457–465. [[CrossRef](#)]
46. Peng, S.; Piao, S.; Ciais, P.; Fang, J.; Wang, X. Change in winter snow depth and its impacts on vegetation in China. *Glob. Chang. Biol.* **2010**, *16*, 3004–3013. [[CrossRef](#)]



© 2018 by the authors. Licensee MDPI, Basel, Switzerland. This article is an open access article distributed under the terms and conditions of the Creative Commons Attribution (CC BY) license (<http://creativecommons.org/licenses/by/4.0/>).